PLANNED YET UNCONTROLLED RE-ENTRIES OF THE CLUSTER-II SPACECRAFT

Stijn Lemmens[(1)], Klaus Merz[(1)], Quirin Funke[(1)] , Benoit Bonvoisin[(2)], Stefan Löhle[(3)], Henrik Simon[(1)]

(1) European Space Agency, Space Debris Office, Robert-Bosch-Straße 5, 64293 Darmstadt, Germany, Email:stijn.lemmens@esa.int
(2) European Space Agency, Materials & Processes Section, Keplerlaan 1, 2201 AZ Noordwijk, Netherlands
(3) Universität Stuttgart, Institut für Raumfahrtsysteme, Pfaffenwaldring 29, 70569 Stuttgart, Germany

ABSTRACT

After an in-depth mission analysis review the European Space Agency's (ESA) four Cluster II spacecraft performed manoeuvres during 2015 aimed at ensuring a re-entry for all of them between 2024 and 2027. This was done to contain any debris from the re-entry event to southern latitudes and hence minimise the risk for people on ground, which was enabled by the relative stability of the orbit under third body perturbations. Small differences in the highly eccentric orbits of the four spacecraft will lead to various different atmospheric entry conditions and are thus predicted to show significantly different behaviour. Given the rare opportunity of a repeatable, predictable, yet uncontrolled re-entry event, and of the object's relatively simple geometries, the definition of multiple in-situ observation campaigns and expected science return in terms of break-up model and risk validation algorithms are explored.

1 INTRODUCTION

International space debris mitigation standards request a permanent clearance of the Low Earth Orbit (LEO) and Geostationary Orbit (GEO) protected regions. Furthermore, the risk on-ground, following a potential atmospheric re-entry, shall be constrained by clear safety limits. Corresponding disposal options are well established for missions in GEO and LEO, and consist of near circular graveyard orbits or atmospheric decay. Science missions, however, sometimes operate on highly-eccentric orbits (HEO) to achieve their mission goals, such as astronomical observations or measurements of the Earth's environment. HEOs describe a group of orbits with perigees in or close to the LEO region and eccentricities above those of Geostationary Transfer Orbits (GTOs) (approximately 0.73). The dominant perturbation forces on these orbits are typically caused by the gravity fields of Sun and Moon.

The European Space Agency's (ESA) Cluster II spacecraft are part of an international collaboration to investigate the physical connection between the Sun and Earth. Flying in a tetrahedral formation, the four spacecraft collect detailed data on small-scale changes in near-Earth space and the interaction between the charged particles of the solar wind and Earth's atmosphere. In order to explore the magnetosphere Cluster II spacecraft occupy HEOs with initial near-polar with orbital period of 57 hours at a perigee altitude of 19 000 km and apogee altitude of 119 000 km. The four spacecraft have a cylindrical shape completed by four long flagpole antennas. The diameter of the spacecraft is 2.9 m with a height of 1.3 m. They are spin stabilised at 15 rpm. The mass amounts to 1200 kg of which 650 kg are propellants, which are expected to be depleted by the end of the mission. After in-depth mission analysis, manoeuvres executed during 2015 will ensure a re-entry of all four spacecraft between 2024 and 2026 [1]. The re-entry epoch can already now be predicted with a high temporal accuracy, of a few days, due to the third body perturbations driving the re-entry, which is in stark contrast to re-entries driven by atmospheric perturbations where a ±20% on the remaining orbital lifetime is considered the standard accuracy [2]. This effectively limits the final re-entry of all four spacecraft to Southern latitudes, minimising the risk for people on ground.

During the past decades space agencies, and more recent space industry and academia as well, have developed software models to evaluate the break-up and demise of spacecraft during re-entries. Due to very limited observational data for validation of these models and the operational needs of the agencies, these models are focussed on re-entries from nearly circular orbits or controlled re-entries. This in turn implies that their usability for atmospheric re-entry from highly eccentric orbit is based on extrapolation, in some cases ignoring the physical differences. This work reviews the limited available observational data on uncontrolled spacecraft re-entries with high flight path angle. It describes the simulated break-up of the Cluster-II spacecraft during re-entry and the associated uncertainties which heavily depend on the exact re-entry conditions. Due to the relatively simple design of the spacecraft, the possibility

Proc. 7th European Conference on Space Debris, Darmstadt, Germany, 18–21 April 2017, published by the ESA Space Debris Office
Ed. T. Flohrer & F. Schmitz, (http://spacedebris2017.sdo.esoc.esa.int, June 2017)

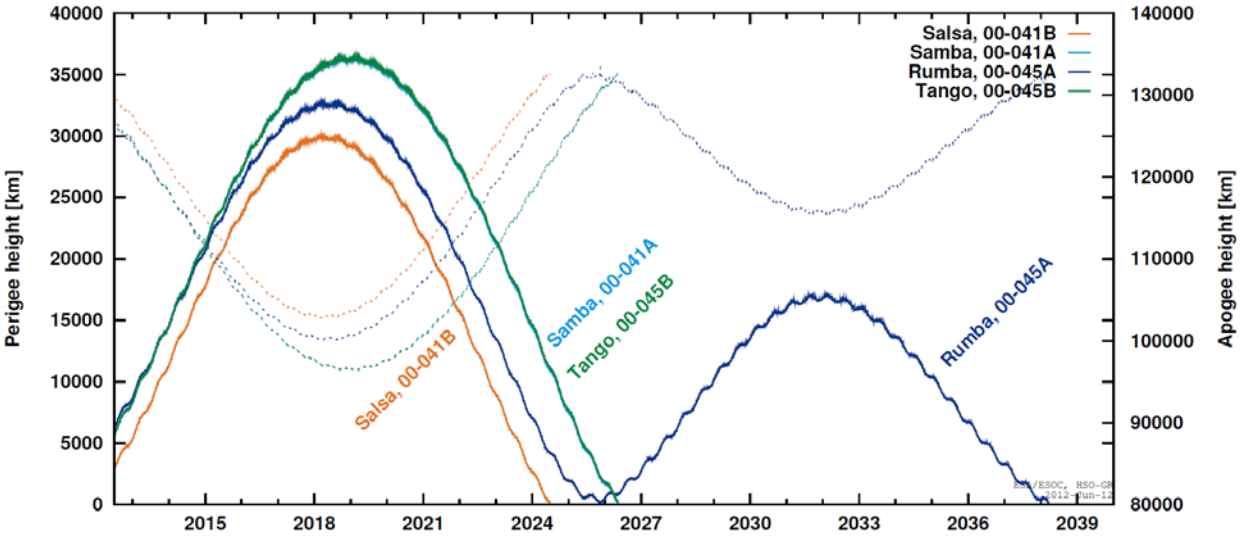

Figure 1 Evolution of perigee and apogee height for the four Cluster spacecraft without manoeuvre.

Table 1. Naming conventions for the Cluster-II spacecraft.

Name	Rumba	Salsa	Samba	Tango
Numbered Name	Cluster-1	Cluster-2	Cluster-3	Cluster-4
Flight Model	FM5	FM6	FM7	FM8
COSPAR ID	2000-045A	2000-041B	2000-041A	2000-045B
US catalogue ID	26463	26411	26410	26464
Predicted Re-entry	2025-11-04	2024-09-07	2026-08-21	2026-08-21

of observing individual component releases, and hence categorising the overall break-up mechanism, is addressed.

2 RE-ENTRY PREDICTABILITY

In order to have a clear naming convention, we will use spacecraft names as given in Table 1 and use the term "Cluster" for the overall mission (i.e. dropping the "II"), in particular Cluster-1 and Cluster-2 will refer to the specific spacecraft and not to the original or recovered overall mission. For Cluster the investigations of re-entry trajectories have a long history and was discussed from 2007, when mission extensions beyond 2010 wre under debate but the orbit of Cluster-2 (Salsa) had to be adjusted as part of the constellation change manoeuvres to avoid the otherwise expected re-entry in spring 2010. The overall constellation change manoeuvres were executed successfully in mid-2010. This led to natural long-term evolutions of the perigee altitude implying re-entries in the years 2024 – 2026 for three of the spacecraft and one in 2038 for the last one (Cluster-1, Rumba). Figure 1 shows the orbital predictions at the time of the mission extension review in 2012.

In the frame of the mission extensions granted in 2012, it was decided to study the orbital evolution and manoeuvre options in more detail and develop models to assess the on-ground casualty risk in case of re-entry. It was obvious that advancing the re-entry of Cluster-1 (Rumba) from 2038 to the mid-2020s would be beneficial to lower the on-ground risk since then the perigee would be located over Southern instead of Northern latitudes. Since shortening the on-orbit time by more than a decade also reduces the risk of an on-orbit collision or break-up, by mid-2014 a baseline strategy for Cluster-1 (Rumba) was selected involving a manoeuvre during the first quarter of 2015 leading to re-entry in 2025 which was subsequently implemented.

The dominating orbit perturbation of these HEOs are the Sun's and Moon's gravity leading to strong variations in the eccentricity, and therefore altitude of perigee since the semi major axis is essentially constant. Secular rates of the orbital elements per orbit averaged over an orbital revolution of the third body are given in [3] and indicate in particular no secular change in semi major axis and a change of the eccentricity resp. perigee altitude depending on the location of the perigee.

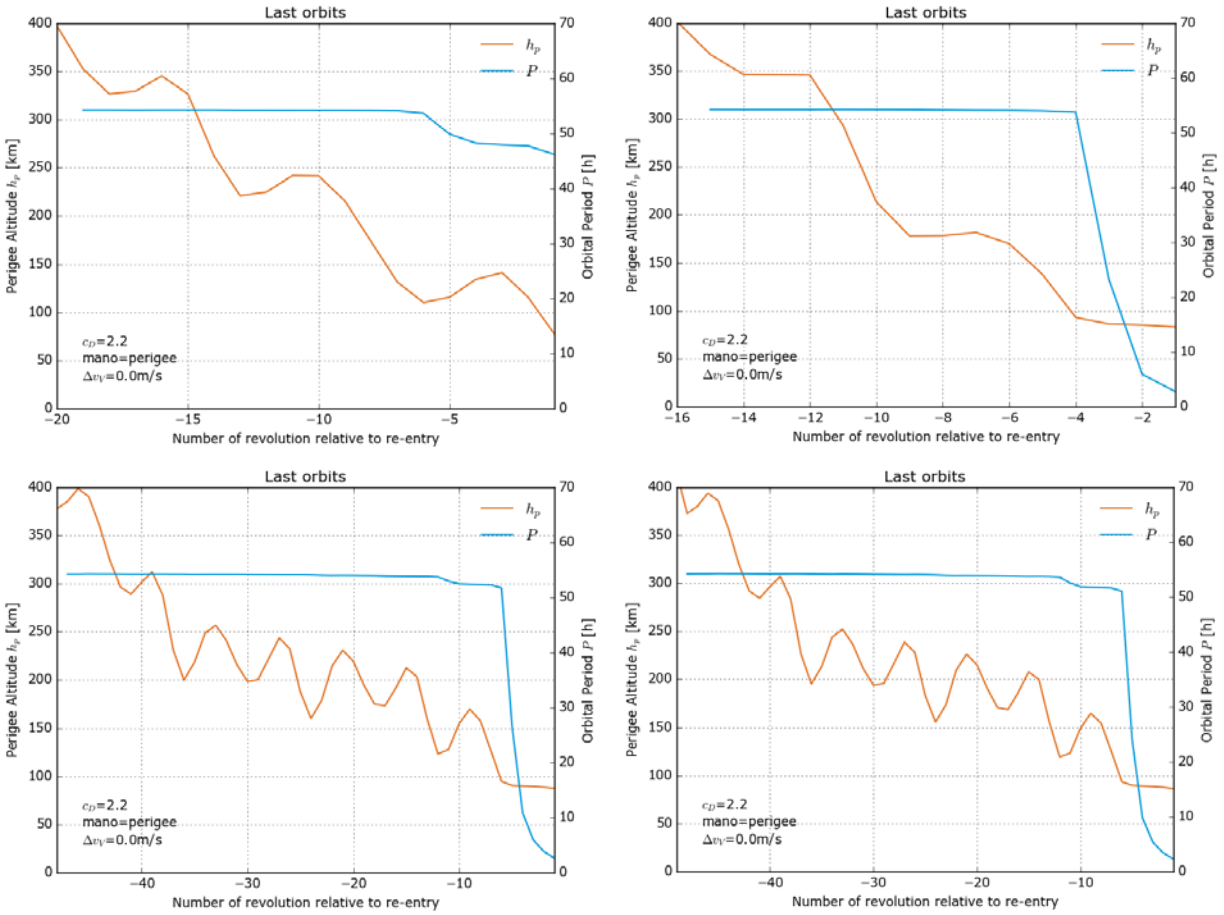

Figure 2 Perigee altitude [km] and orbital period [hours] for the last perigee passages before re-entry for Cluster-1 (top left), Cluster-2 (top right), Cluster-3 (bottom left) and Cluster-4 (bottom right) based on a full numerical prediction extending an operational orbit of 2016

For the argument of perigee (measured with respect to the third body's orbital plane) being in the 2nd or 4th quadrant the eccentricity decreases and the perigee altitude increases, whereas eccentricity increases and perigee altitude decreases for the argument of perigee being in the 1st or 3rd quadrant. The secular effect due to the Moon is about double the effect due to the Sun. Long-periodic effects are described in [3] as well, with a period of half the orbital period of the third body, i.e. half a year for the Sun and approximately two weeks for the Moon. For the long-periodic oscillations the effect of the Sun is about six times larger than that of the Moon in terms of amplitude of eccentricity or perigee altitude and can reach about 200 km due to the Sun perturbation and some 10s of km due to the Moon.

These analytical considerations are useful to understand the overall evolution, however for a detailed analysis a higher order semi-analytical or full numerical propagator is required. This is particularly true for the evolution of the perigee altitude during the last few orbits before actual re-entry: The combination of all perturbations may lead to a slow or fast decrease of the perigee altitude during these final revolutions depending on whether the long-periodic and higher order effects nearly cancel each other or are amplified by superposition in which case the perigee altitude of the last orbits may reach several 10s of km difference from one orbit to the next. In case the pattern is steep enough, the object will enter the deeper layers of the atmosphere without first circularizing its orbit, as is usually the case for the more typical uncontrolled re-entries from lower orbits.

Since then the breakup occurs near the location of the perigee, this would allow predicting and therefore potentially controlling the latitude band of the break-up process and therefore limiting the distribution of fragments on ground in terms of latitude. Even more, if the orbital period could be controlled precisely at EOL and is not perturbed by air drag until the very last revolution, one may even predict and control the time of the re-entry and therefore the sub-satellite longitude of the final perigee and therefore the longitude range of the fragments reaching ground. This is illustrated by Figure 2 showing the decrease pattern of the last perigee altitudes for the 4 Cluster spacecraft propagated from their current operational orbit. The top plots for Cluster-

1 and -2 show a steep pattern where the perigee altitude decrease towards the end is about 50 km per revolution. For Cluster-1 (top left plot) the last large step in perigee altitude is desirable from an on-ground risk point of view. To the contrary Cluster-2, while also showing a steep decrease, shows a perigee pass at an altitude of about 90 km which leads to large reduction in orbital period and therefore weak lunisolar perturbations during the remaining revolution(s) with a perigee altitude evolution driven primarily by air drag It has, however, to be noted that any particular scenario like this is to be considered as an unreliable prediction as long as no proper break-up model is used but a standard three degrees of freedom (3DOF) numerical propagator with extensive environment options enabled. The lower two plots show the situation for Cluster-3 and -4 which are on very similar orbits. For them the secular decrease and the Sun-induced long-periodic oscillation essentially cancel during some 10 to 40 revolutions before re-entry, leaving essentially the biweekly wobbles due to the moon.

In [2], the stability of these re-entry point predictions w.r.t. unknown or variable properties of the objects, such as reflection and drag coefficient, and operational scenarios, such as the influence of orbit control manoeuvres and attitude motion at the end of a passivation phase, are analysed. The spread on the re-entry epoch for a given initial epoch is in the order of one day and typically dominated by the variation of the drag coefficient. This indicates that precise timing and therefore control of the longitude of the debris-fallout zone is not possible seven years before re-entry. In order to assess if this uncertainty can be reduced when we are nearing the nominal re-entry date, and hence to assess the feasibility of an airborne re-entry campaign for these uncontrolled re-entry events, the following analysis is performed:

- A reference trajectory for the re-entry of each spacecraft by extending the nominal mission plan, which has predictions up to 2021, by propagating the nominal mission parameters.
- Orbital states are sampled from these trajectories at the beginning of 2017 and 2 months before predicted re-entry.
- These states are perturbed by an impulsive manoeuvre of uniformly sampled delta velocity size but limited to 25cm/s in 2017 and 8.6 cm/s in the year of re-entry. This is included to mimic conservatively the effect of a potential battery leakage.
- These states are also perturbed by a uniformly sampled initial drag coefficient (assuming a cannonball model) limited to the interval [1.1, 4.4] in 2017 and [2.0, 2.4] in the year of re-entry. This is included to mimic the uncertainty in the attitude motion, the thermosphere conditions, and the intrinsic uncertainty of the drag coefficient, where the first one can be reduced by observation closer to the re-entry and the last two remain. The effect of the thermosphere density is only relevant when prolonged circularisation is expected.
- A hundred samples are drawn to ascertain the spread in longitude and possibility of qualitative re-entry behaviour change.

The results of this sensitivity analysis are added in Annex A, Figure 11 to Figure 14. The top two subfigures for each Figure depict the evolution of the perturbed orbits' perigee altitude and orbital period w.r.t. the revolution number prior to re-entry, in this case defined as the revolution in which the 3DOF propagation reaches state below 50km in geodetic altitude. The bottom subfigure shows the ground-track for the re-entry trajectory which meets the stopping criteria from a geodetic altitude of 150km down to ground impact. Each symbol-line represents a unique initial sampled state.

The simulations started for the four spacecraft in 2017 show the behaviour expected from the theory outlined earlier: the randomised manoeuvre leads to a change in orbital period which makes the longitude point essentially spread around the globe whereas the change in drag coefficient matters for the behaviour of re-entry itself when the perigee altitude drops below approximately 100km. In case of Cluster-1 and -2, this makes the difference between a direct re-entry and limited circularisation. The reference for Cluster-3 and -4 was already in a state of limited circularisation and these sampled results do not indicated that the situation would qualitatively change when considering perturbations.

In the simulations for the four spacecraft when started two months prior to the reference trajectory indicate that the spread in longitude reduced to between 25% and 33% of the longitude band at the perigee point. These distances, taking into account that the uncertainty reduces further when considering times closer to re-entry, are already within limits of current airborne re-entry observation campaign concepts [4]. This would however imply a change towards a more dynamic planning, where different starting scenarios and observational geometries are considered depending on the orbit evolution during the last weeks prior to re-entry. Circularisation cases, depending on the drag coefficient and to a lesser degree that state of the thermosphere, are still present for Cluster-1, -2, and -4, which could trigger a spread of fragments to different latitudes. In case of an operational Cluster mission right until re-entry, which currently is at least technically feasible, the uncertainty on the drag coefficient, and the prediction errors such as attitude motion which it could absorb, would be known and the impact location would

become predictable with increasing accuracy. These conclusions apply to the first entry of the spacecraft through geodetic altitudes below 100km, where the 3DOF approximation breaks down for accurate phenomenological assessment of the object's behaviour. Concretely, the effects of aerothermal loads and structural mechanics under the rising dynamic pressure on the object can no longer be ignored

3 OBSERVING RE-ENTRY BREAK-UPS

In general the amount of dedicated observation campaigns to study re-entry break-up events, be it via on-ground, on-orbit, or in-situ sensors, is surprisingly low given that on average an object with mass above one ton re-enters the Earth's atmosphere every two weeks. For the purpose of this study, we are interested in the derived break-up altitude from such observations to see if a correlation with the initial orbital parameters can be established.

The first systematic analysis into the break-up process was conducted during the early 70'ies by the United States Air Force under the Vehicle Atmospheric Survivability Project driven by the need to distinguish ballistic warheads from decoys and re-entering rocket stages [5]. Six satellite re-entries were extensively tracked by tracking aircraft, tracking ships, and ground-based sensors equipped with radar, optical, and spectrographic instruments. The first four featured a specific type of satellite, weakly attached to an Agena-D upper stage, and are collectively referred to as VAST (Vehicle Atmospheric survivability Tests). The last two featured a large optical payload satellite of the monocoque Keyhole type which are referred to as VASP (Vehicle Atmospheric Survivability Project). From the four VAST tests, the lack of significant impact on the break-up of the actual re-entry attitude of the objects is notable. The main break-up of the objects occurs between 81 and 75 km in geodetic altitude. From the two VASP re-entries the main break-up sequence, excluding low ballistic coefficient objects such as solar panels, occurs between 85 and 75 km in geodetic altitude, peaking at 78 km. A further two re-entries from highly eccentric orbits in 1996, and two controlled deorbited satellite in 1997 and 2000 have been reported as showing heating and break-up in line with the VAST and VASP tests, however no figures could be retrieved from public sources. Further radar and optical observations have been obtained from the ballistic re-entry of Ariane 5 EPC (Etage Principal Cryotechnique) stages. The more conclusive results indicate a first major break-up of the hydrogen tank between 68 and 66km in geodetic altitude [6].

On the 23rd of March 2001 the MIR space station was deorbited over the Pacific ocean. This has been recorded with conventional camera equipment and this data was analysed to derive the break-up conditions [7]. Mechanical break-up of the station modules is postulated to have taken place, at 76km, before thermal fragmentation becomes the break-up driver until 69 km.

Multiple so-called break-up recorder have been developed and deployed during this decade, i.e. the REBR(-W) (REentry Break-up Recorder), I-Ball, and BUC, which aim at making in-situ observations of the acceleration, pressure and temperature during a re-entry event. These sensors have been installed on cargo vessels for the International Space Station. Of the seven models used to date, three REBR models have consistently returned break-ups between 77 and 67km in geodetic altitude when deployed on two HTV and one ATV cargo vessels [8].

Airborne re-entry campaigns executed during the last and current decade have become a prime source for spectrographic data on re-entry break-up events. Leveraging on the communalities between the observations of meteoroid showers and those of man-made space object re-entries, spectrographic techniques have been used to attempt fragment identification and re-entry environment characterisation [4]. Both the ability of tracking individual objects within a fragmentation debris cloud as well as obtaining the integrated result over a cloud has been demonstrated. The controlled re-entry of the ATV-1 in 2008 showed a major fragmentation within the main events timeline between 83 and 71km in geodetic altitude [9]. Re-entry observations where made from JAXA's Hayabusa re-entry capsule in 2010. Even though the observations were focussed on the surviving capsule, the break-up of the spacecraft is visible in the data. As far as known to the authors the break-up of the main spacecraft bus, which separated 80 minutes prior to the superorbital velocity re-entry from the capsule, has not been computed from the data. Within the scope of this work, the break-up has been estimated to occur between 78km and 65km in geodetic altitude when observations are compared to the reference case [10]. In 2015 a presumed space debris object WT1190F returned to Earth on an eccentric orbit with a superorbital entry speed of 10.61 km/s, relative to the atmosphere at 100 km altitude, and an entry angle of 20.6°. The main fragmentation was estimated between 58km and 45km in geodetic altitude. Similarly the controlled re-entry of a the Cygnus OA6 spacecraft was observed during 2016, with the preliminary analysis suggesting that the main break-up takes place between 80km and 72km.

The earlier tests served as input for on-ground casualty risk estimation methodologies. These methodologies assume a thermo-mechanical break-up of the outer spacecraft with the sequential release of the inner-spacecraft components. At 78km geodetic altitude is the

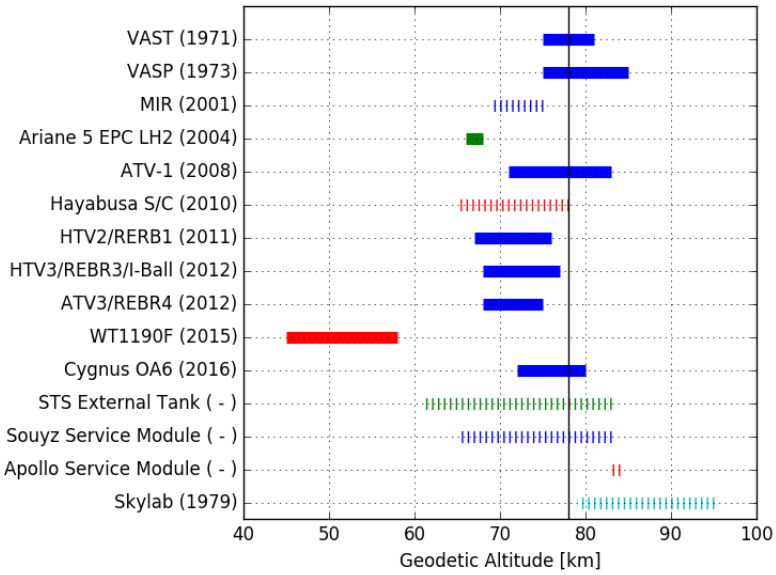

Figure 3:Comparison of main break-up altitudes for the observed re-entries of man-made objects. Blue: controlled de-orbits, Green: ballistic trajectory, Red: Superorbital re-entry velocities, Cyan: (psuedo-)uncontrolled. Solid lines indicated direct observation of the break-up parameters, dashed lines indicate missing data on part of the trajectory, preliminary assessment, or missing data on the methodology used.

internationally accepted and defacto standardised break-up point for risk evaluation. The overview is presented in Figure 3. This indicates that the 78km boundary is a reasonable match for the available controlled re-entry data but a large spread can be observed, especially for re-entries with superorbital velocities (and generally steep flight path angles). The last four data entries are included from [12], but methodologies used to obtain them could not be retrieved. The high break-up of the Skylab re-entry could be in line with the postulated high altitude break-up of MIR, driven by mechanical rather than thermal failure, but solid observational data is missing. The reported high altitude break-up of the Apollo service module, could be due to the relative lightweight design, even though a larger spread would be expected. In terms of design, only the VASP and Hayabusa spacecraft are somewhat representative for the general spacecraft population which could pose a risk to people on ground.

4 BRIDGING THE GAP BETWEEN OBSERVATION AND PHYSICS

Deriving the science of re-entry break-ups can be tackled by two complementary approaches. The observational approach, outlined briefly in the previous section can be further augmented by analysis of on-ground impacting fragments, for which a detailed overview is beyond the scope of this work. On the other side, bottom up physics or first principles approaches require in-depth knowledge of the material characteristics making up the object, understanding the aerodynamics and heat-transfer associated to the rarefied regime, describing the mechanical loading and stresses acting on the spacecraft at high temperatures and chaotic attitude behaviour, and confident predictions on the trajectory and attitude behaviour of fragments during a break-up. Both approaches are currently far apart, given the complexity of modelling a full spacecraft with physics based modelling and taking into account all fluid dynamical and chemical aspects on one hand, or deriving unambiguous data from observation which would enable fragment identification beyond lose material associations on the other hand.

Driven by the practical need of on-ground casualty risk estimation for the re-entry of man-made objects, software has been developed since the 1990'ies to bridge the gap between observations and first principles. So called object-oriented tools model spacecraft as a collection of individual geometric shapes for which analytic formulas approximately describing trajectory and heating on these objects are available. Their main benefit is methodological risk assessment based on clear procedures and their computational efficiency which allows parametric analysis. So called spacecraft-oriented tools model the object in a finite elements approach (limited to major components and not down to the screws and bots) and implement simplified aero-thermal and mechanical numerical algorithms to predict the break-up and identify the surviving fragments. Simplifications w.r.t. full computational fluid dynamics (CFD) analysis is still required to obtain results in reasonable run-times for full spacecraft (in the order of.

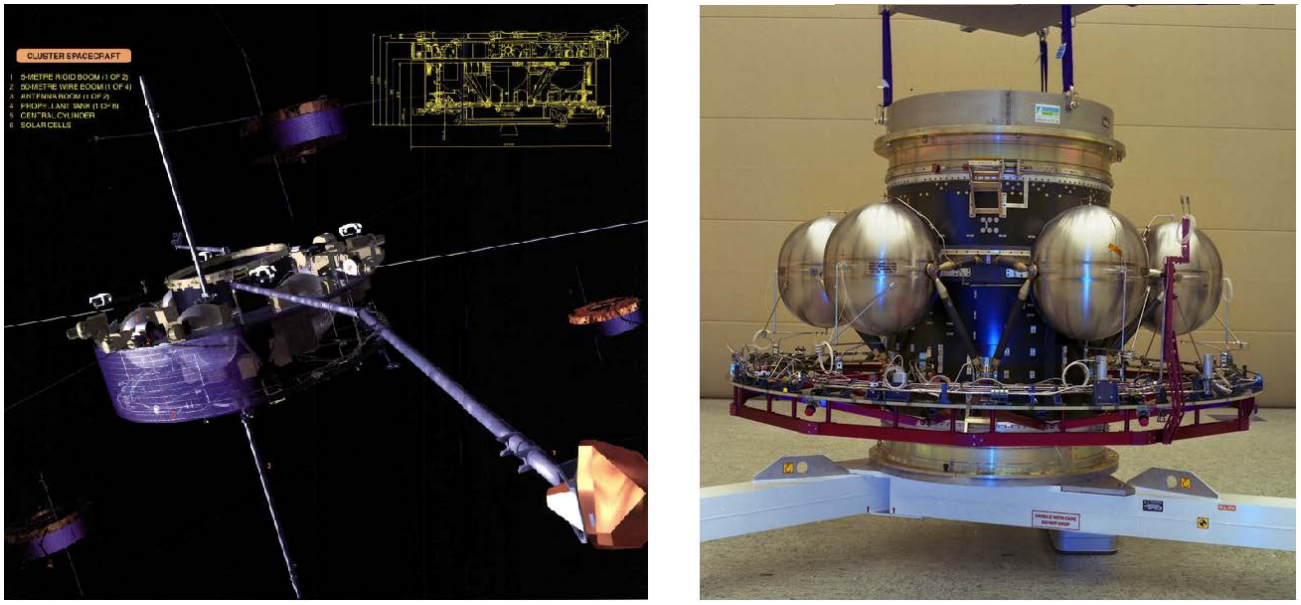

Figure 4: Cluster spacecraft overall design(left) and close up on the central cylinder (right).

days for current commercial desktop hardware). Both type of tools provide output which can be qualitatively verified against observational data by the forward modelling approach [13]. It is important to stress that these tools are developed with phenomenological accuracy in mind and accept the limitations in physical accuracy which stem from the approximations used.

To provide further validation for the risk assessment tools and to identify the main physical drivers to describe the real-world break-up, the need to numerically rebuild a re-entry event and provide measurable scientific predictions beyond the break-up altitude or confirmation of material types released becomes pressing. This has been long the case for controlled re-entries of both manned and unmanned re-entry capsules based on CFD analysis, but is largely absent for uncontrolled re-entries. The problem of deterministically rebuilding the full re-entry event is complex for objects which were designed for it, and unfeasible for uncontrolled re-entries due to the chaotic attitude motion and non-deterministic break-up of spacecraft parts. Therefore, one step forward to cross between physics based models and observations would be the identification of markers which are expected during the re-entry event and can be more confidently modelled using an object- or spacecraft-oriented approach.

The Cluster mission will remove part of the uncertainty on the re-entry trajectory which is associated in general with uncontrolled re-entries, in part due to the fairly predictable translational orbit dynamics as seen in the previous section, and in part due to the stable attitude motion of the rotating spacecraft which maintains its rotation axis under the environment perturbations until re-entry. Moreover, top-level the design of the spacecraft is relatively uninvolved. The spacecraft's cylindrical design is driven by the body-mounted solar array and also optimises the fields of view available to the experiments, which are accommodated on the main equipment platform on the upper side of the spacecraft. The compact spacecraft primary structure provides mass-efficient load paths to the mechanical interfaces. It consists of the central cylinder, the main equipment platform, a tank support structure, a platform internal to the central cylinder and a Reaction Control Subsystem (RCS) support ring. The central cylinder is fabricated as a CFRP skinned aluminium honeycomb sandwich, and the Main Equipment Platform (MEP) as an aluminium-skinned honeycomb panel reinforced by an outer aluminium ring. The MEP is supported by symmetrically arranged CFRP struts connected to the central cylinder. Six cylindrical titanium propellant tanks with hemispherical ends are each mounted to the central cylinder via four CFRP struts and a boss. A further in-depth description on the design is available in [14] but here we will focus on the propellant tanks.

Propellant tanks, or in general pressure vessels, are commonly identified as remainders of re-entry break-up events when found on-ground. As of January 1st 2017, they account for 95 out of 162 objects (excluding the re-entries of Columbia STS, Skylab, and Salyut 7) [15].

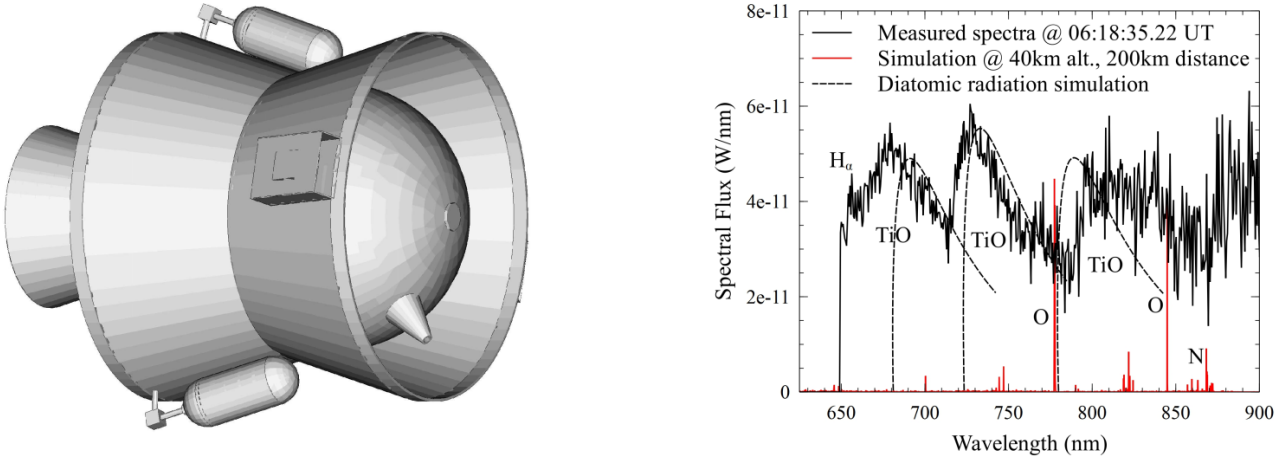

Figure 5: Trans Lunar Injection Stage candidate for WT1190F identification as SCARAB model (left) and observed spectrum during the WT1190F re-entry with the identification of TiO bands (right).

Out of these 41 are pure titanium allow shells, 34 belonging to rocket bodies and 7 belonging to satellites. A recurring element in this group is the casing associated to the Star 48B apogee kick motor. For which detailed post-re-entry analysis has established to oxidation of the outside surface of the casing [16]. These phenomenological observational findings are well in line with the on ground testing of titanium alloys in wind tunnels and solar furnaces which are aimed a mimicking approximate environment conditions during re-entry [17-19]. All tests, under different conditions and in different facilities, indicate the formation of TiO_2 with various degradation modes such as peeling of and cracking. The formation of TiO_2 both as rutile and anatase have been observed under temperature conditions as low as 700K, but general formation conditions depend on pressure conditions and chemical composition of the plasma as well. Moreover, this has a time dependence component as the thickness of the oxide layer depends on the environmental exposure time.

The formation of TiO_2 by itself is important for re-entry break-up models, as it affects the surface emissivity and hence the radiative cooling of a titanium object during re-entry. At high temperatures, above 1500K, TiO_2 and Ti will further react to form titanium monoxide TiO [20], which as a free molecule will produce a molecular band spectrum in visible wavelengths due to its vibrational motion [4]. Even though not the main point of attention, TiO was observed as part of the plasma wind tunnel demisability of titanium samples [17]. These bands have been tentatively observed via spectroscopy measurement of the WT1190F [11]. It is important to stress that there is no direct evidence that this object is man-made, but only circumstantial derived evidence from its orbital behaviour. In order for the TiO to be observed without clutter from Aluminium Oxide bands which are more commonly associated with re-entry spectra [4], a free flying component of titanium basis, such as an titanium alloy tank with molten attachment points, would have to be present and reach the required temperatures.

A candidate object identified is the insertion stage of NASA's Lunar Prospector mission [21], which is essential a STAR 37 FM solid rocket motor engine with extended functionality, as before. In order to assess if the required temperature could be reached, the stage was modelled with ESA's spacecraft-oriented tool SCARAB 3.1L. SCARAB has been developed under ESA contracts since 1995, under the lead of HTG (Hypersonic Technology Göttingen) and with support from other European and international partners [22]. During the re-entry simulation the heat flux peaks within 20 seconds to over 6000 kW/m^2 for a geodetic altitude between 90 and 40 km. This leads to the melting temperature of titanium being reached between 50 and 60km and sustained for a couple of seconds. Only the STAR 37 FM motor remains while the stage fragments thermally. Tentatively TiO could form on this object and explain the observation at an altitude of 40km in Figure 5. However, a detailed thermochemical analysis would be required to validate this postulate.

The use of the six titanium tanks of each the four Cluster spacecraft are hence proposed as markers during a re-entry campaign. They constitute a class of objects which are generally found to survive the re-entry as single entities [23,24], i.e. without structural attachment points, and hence constitute a single material object close to the capabilities of computational models and observational techniques. The different re-entry geometries of the individual spacecraft yields a set of 32 repeated object samples under 4 distinct environment conditions

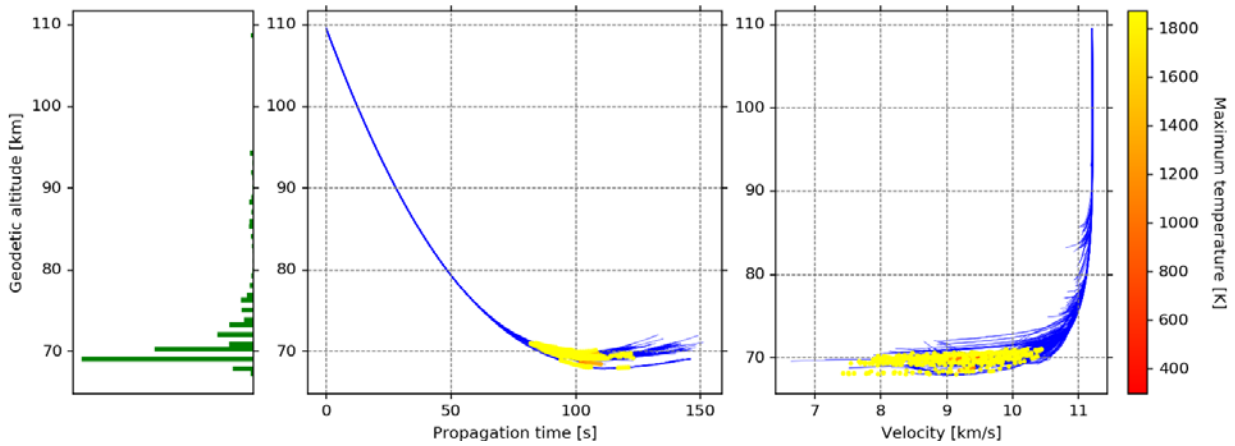

Figure 6: Re-entry break-up simulations for Cluster-1.

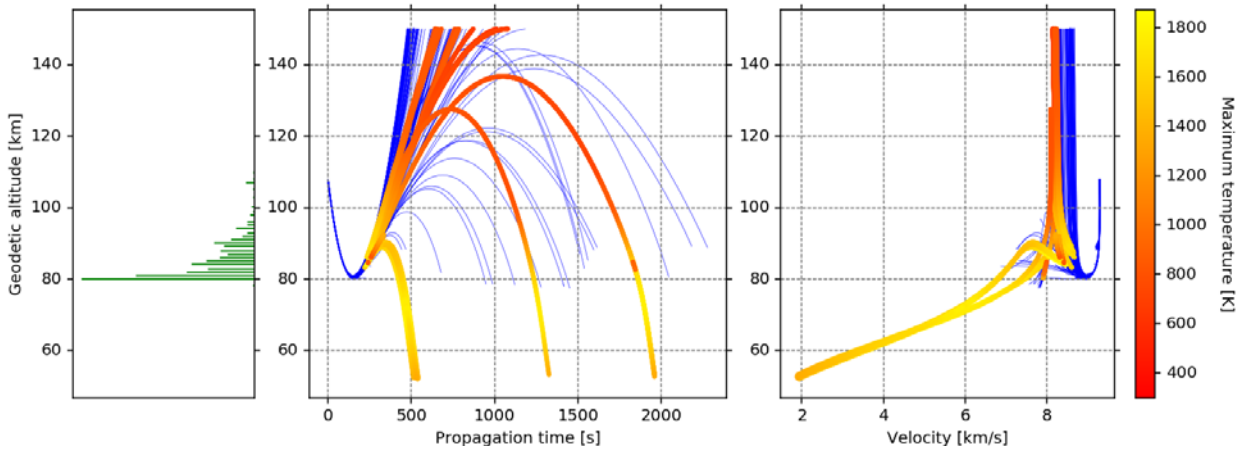

Figure 7:Re-entry break-up simulations for Cluster-2.

5 CLUSTER-II BREAK-UP MODEL AND PREDICTION

A detailed SCARAB model was already developed for the Cluster spacecraft when assessing the on-ground risk during the disposal manoeuvre planning [25]. The study takes off where the 3DOF approximations of Section 2 reach their limits. This leads to the need to follow escaping fragments for the purpose of risk assessment and the identification of theoretical break-up behaviour depending on the initial orbital conditions. In this work we will re-use the model to derive the predicted behaviour of the propellants tanks for the four reference scenarios. The following caveats need to be observed:

- As the re-entries are only predictable for the first destructive contact with the atmosphere, the follow-up on escaping fragments is omitted here.
- The deterministic break-up simulations are repeated with ten different feasible initial attitude conditions to randomise the results.
- SCARAB implements Lees correlations for convective heat flux. For high velocity re-entries this is a conservative limit w.r.t. demisability.
- Structural fragmentation of the spacecraft is only considered for the antennas and booms of the spacecraft.

The results of the SCARAB break-up simulations for the four spacecraft are given in Figure 6 to Figure 9. All of those figures will depict in the left most plot a histogram which provides the normalised distribution of fragmentations events of the model during the simulation. It is a proxy for the break-up altitude represented in Figure 3. The remaining two plots depict the trajectories of all fragments created during the ten simulations per spacecraft and their evolution in terms geodetic altitude versus time (centre) and geodetic altitude versus velocity (right). Blue trajectories are any type of fragment; trajectories shown by a colour gradient between yellow and red correspond to fragments which are predominantly part of the titanium

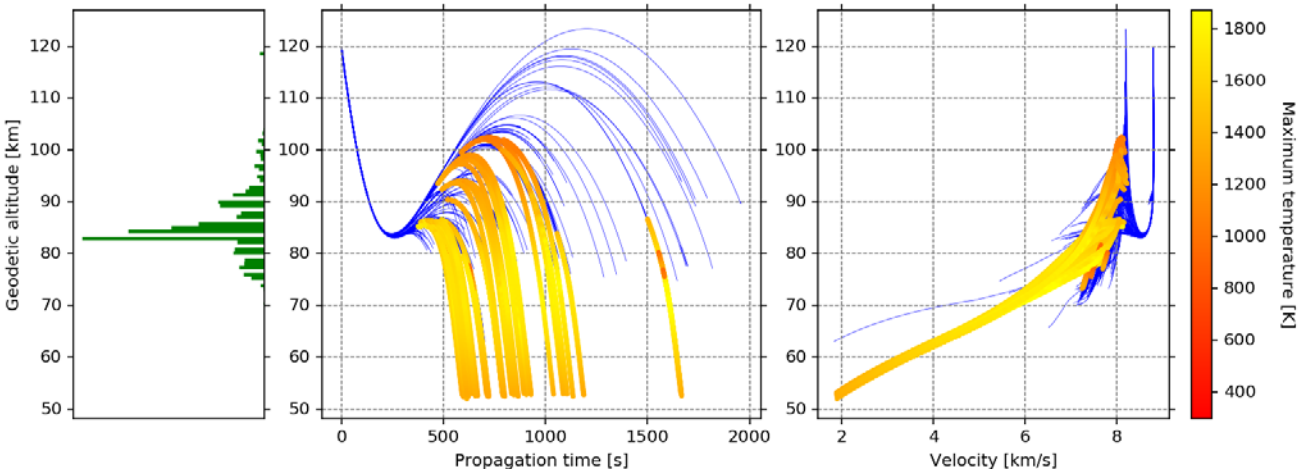

Figure 8: Re-entry break-up simulations for Cluster-3.

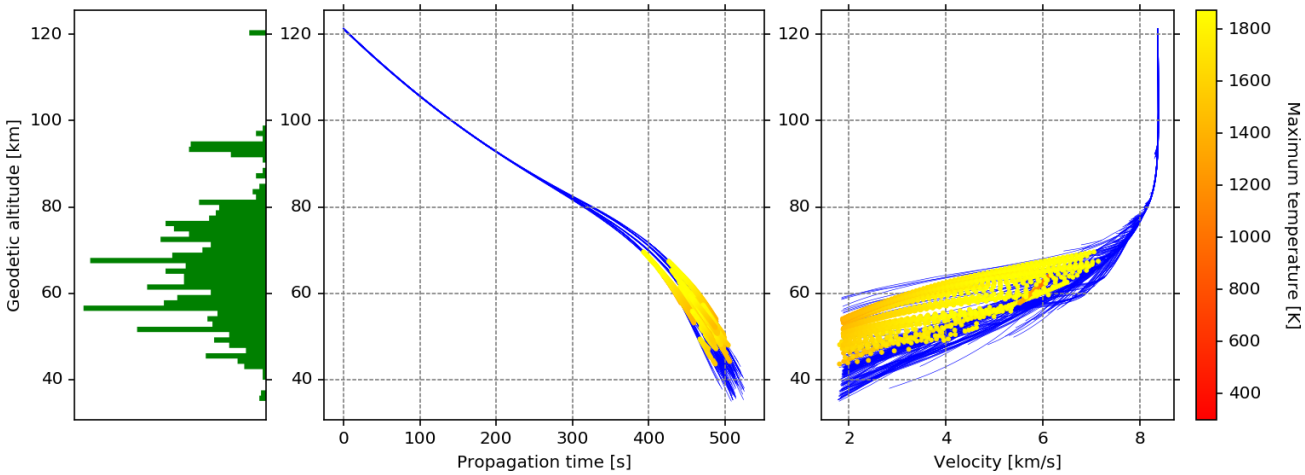

Figure 9: Re-entry break-up simulations for Cluster-4.

propellant tanks. The colour bar for these propellant tanks, or fragments thereof, ranges between 300K and 1873K. The former is the initial temperature of the spacecraft during the re-entry simulation and the latter one the melting temperature of the modelled titanium allow (TiAl4V6).

In all simulations Cluster-1 ‘hits’ the narrow zone identified in [25] where the spacecraft demises fully, including all titanium tank fragments. The geodetic altitude zone where this happens, between 75 and 68km is characterised by high velocities which are more common for superorbital re-entries. By the time the tanks break free from the parent spacecraft, they are already at melting temperature. In the case of Cluster-2, the geodetic break-up altitude regime between 90km and 80km is too high up for the spacecraft to re-entry but high enough to trigger the break-up. In most cases, not fragments impact on ground but continue on orbital trajectories when not demised (in terms of risk analysis this objects are tracked and re-analysed upon the next entry after an orbital revolution). When tanks fragments do not manage to reach orbital velocities, they are not predicted to melt either. This would enable long trajectories potentially crossing again into the higher layers of the rarefied regime to be observed while the tanks still have high maximum temperatures. Cluster -3 shows the same tendencies as for Cluster-2, however none of the fragments escape and the trajectories for the propellant tanks, or fragments thereof, are actually representative for the re-entry of a ‘standard’ object from low Earth orbit in terms of altitude and velocity profile, albeit starting at a higher initial temperature but still without melting. The main break-up events take place between 90 km and 75km in geodetic altitude. The case of Cluster-4 is one of a steep re-entry, with the main fragmentation taking place between 80 km and 50km in geodetic altitude. In all simulations, all fragments were contained and follow the path of a re-entry with elevated flight path angle but with moderate

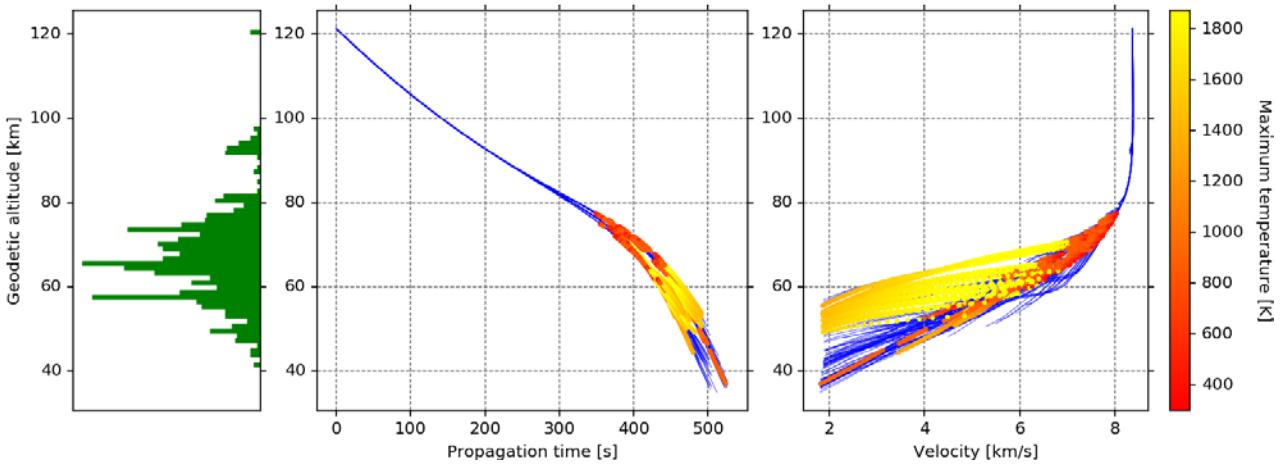

Figure 10: Re-entry break-up simulations for Cluster-4 with modified break-up criterion for the propellant tank struts.

velocities. All propellant tanks, and fragments thereof, are predicted to impact on ground.

The case of Cluster-4 allows an additional question to be addressed, namely to address to which degree thermal and structural fragmentation are coupled. As seen for large structure, early mechanical fragmentation is expected. In the case of Cluster, the struts holding the tanks in place are designed to support them under vertical launch loads and horizontal rotation, not the full chaotic attitude mode for the spacecraft during re-entry. In the previous simulations, the tanks break free when either the Aluminium connectors or CFRP struts are starting to melt. A separate break-up criterion at lower temperatures is added to the struts in order to simulate an early break-up. This is shown in Figure 10. The overall behaviour of the break-up is expected to remain the same, however the signature of the tanks would be individually detectible at higher altitude. However, the analysis of potential failure modes of the struts under re-entry conditions would need to be analysed in depth.

6 CONCLUSIONS

The re-entry of the four Cluster spacecraft between 2024 and 2026 provide a unique opportunity to observe the re-entry of identical object under significantly different atmospheric entry conditions. Under the current operational orbit plan, representative trajectories for superorbital entries as well as ‘standard’ re-entries from Low Earth orbit can be identified for the fragments. The rotationally stable attitude motion of the spacecraft will lead to homogenous heating and hence simplify the initial break-up dynamics. The six propellant tanks per spacecraft are identified as suitable candidates for dedicated tracking during the re-entry break-up events as they are likely to survive, have a shape and single material properties within computational reach of both the CFD models and risk analysis tools, and show the potential of multiple spectrographic signatures to serve as proxies for the chemical environment.

Further components of the spacecraft could be investigated for the use as marker, e.g. the Nickel-Cadmium batteries, however the return in terms of phenomenological understanding of a break-up for eccentric orbits would be on the par with the VASP project, which continues to define the risk analysis standards to this day.

7 REFERENCES

1. Merz, K., Krag, H., Lemmens, S., Funke, Q., Böttger,S., Sieg, D., Ziegler, G.,Vasconcelos, A., Sousa, B., Volpp, H.-J., Southworth, R. (2015), Orbit Aspects of End-Of-Life Disposal from Highly Eccentric Orbits, *Proceedings of the 25th International Symposium on Space Flight Dynamics, München, Germany*.

2. Merz, K., Lemmens, S., Funke, Q., Frey, S. (2016), Optimization of End-Of-Life Disposal Maneuvers for Highly Eccentric Orbits, *Proceedings of the AIAA/AAS Astrodynamics Specialist Conference, AIAA SPACE Forum, (AIAA 2016-5513)*.

3. Eliasberg, P. E. (1965), *Introduction to the Theory of Flight of Artificial Earth Satellites*, Moscow, Nauka, p.491.

4. Löhle S., Zander F., Lemmens S., Krag H., (2017), Airborne Observations of Re-entry Break-up Results and Prospects, *Proceedings of the 7th European Conference on Space Debris, Darmstadt, Germany*.

5. Stern, R. G. (2008). Reentry Breakup and Survivability Characteristics of the Vehicle Atmospheric Survivability Project (VASP) Vehicles. *AEROSPACE REPORT NO. TR-2008(8506)-3*.

6. Lips, T., Fritsche, B., Koppenwallner, G., Leveau, C.

(2007), Ariane-5 EPC Re-entry – A Comparison of Observations and Scarab Simulation Results. *Proceedings of the 2nd IAASS Conference*.

7. Stern, R. G. (2003). Analysis of Mir Reentry Breakup. *AEROSPACE REPORT NO. TR-2003(8506)-1*.
8. Feistel, A. S., Weaver, M. A., Ailor, W. H. (2013), Comparison of Reentry Breakup Measurements for three Atmospheric Reentries. *Proceedings of the 6th IAASS Conference*.
9. Bastida Virgili, B., Krag, H., Lips, T,. De Pasquale, E. (2010). Simulations of the ATV Re-entry Observations. *Proceedings of the 4th IAASS Conference*.
10. Grinstead J., Jenniskens, P., Cassell, A., Albers, J., Winter, M. (2011), Airborne Observation of the Hayabusa Sample Return Capsule Re-entry. *Proceedings of the 42nd AIAA Thermophysics Conference, Fluid Dynamics and Co-located Conferences.*
11. Jenniskens, P., et al. (2016). Airborne observations of an asteroid entry for high fidelity modeling. *Proceedings of the 54th AIAA Aerospace Sciences Meeting*.
12. Herdrich, R. J., Nguyen, P. D. (1997), Super Lightweight Tank (SLWT) Footprint Analysis: Technical Report. *NASA Johnson Space Center, JSC-27712*.
13. Lemmens, S., et al. (2016), From End-of-Life to Impact on Ground: an Overview of ESA's Tools and Techniques To Predicted Re-entries From the Operational Orbit Down to the Earth's Surface. *Proceedings of the 6th ICATT Conference*.
14. Mecke, G. (1995), The Cluster Spacecraft: A Unique Production Line, *ESA bulletin 84, European Space agency*.
15. ESA, ESA's Re-entry Predictions (consulted 2017-01-01), Online at *https://reentry.esoc.esa.int*.
16. Steckel, G. L., (2016). Summary of Reentry Effects on Five Delta II Upper-Stage Star 48 Motor Cases. *AEROSPACE REPORT NO. TOR--2016--02193* .
17. Schleutker, T., (2016)., Final Report: Characterisation of Demisable Materials (CHARDEM), *European Space Agency 4000110952/13/NL/CP*.
18. Balat-Pichelin, M., Omaly, P., (2015). Study of the Atmospheric Entry of Metallic Space Debris: Oxidation and Emissivity Evaluation to Contribute to Design for Demise, *Proceedings of the 8th European Symposium on Aerothermodynamics for Space Vehicles.*
19. Prévereaud, Y., Véranta, J.-L., Balat-Pichelin, M., Moschettac, J.-M., (2016). Numerical and experimental study of the thermal degradation process during the atmospheric re-entry of a TiAl6V4 tank, *Acta Astronautica, Volume 122, Pages 258–286*
20. Holleman, E., Wiberg, N. (2007). *Lehrbuch der Anorganischen Chemie*, Berlin – New York, de Gruyter, Issue 102, p. 1530.
21. Andolz, F. J (1998). Lunar Prospector Mission Handbook, *Lockheed Martin Missiles and Space, LMMS/P458481*.
22. Lips T.,et al. (2007). Reentry Risk Assessment for Launchers Development of the New SCARAB 3.1L, *Proceedings of the 2nd IAASS Conference.*
23. Durin, C., et al. (2013). Study of Spacecraft elements surviving an atmospheric Re-entry, *Proceedings of the 6th IAASS Conference.*
24. Lemmens, S. (2016). Spanish recovered space objects - current status of investigation, *ESA Report GEN-REN-ME-00182-HSO-GR.*
25. Kanzler, R., (2014). Re-entry from Highly Eccentric Orbits – Cluster-II, *6th International Astronautical Congress*.

8 ANNEX A: REENTRY LONGITUDE UNCERTAINTY ANALYSIS

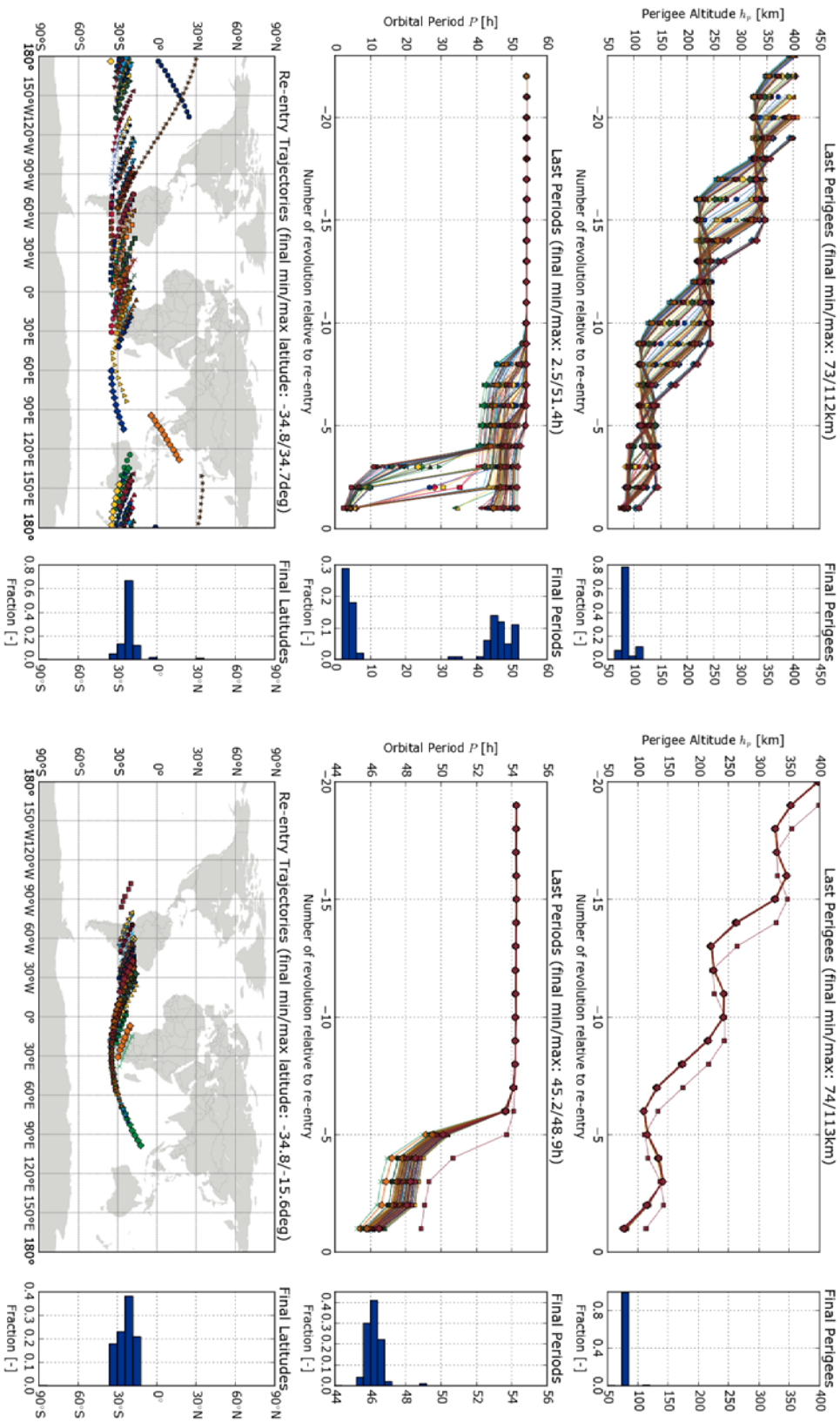

Figure 11: Re-entry longitude analysis for Cluster-1, starting from January 2017 (top) and September 2025 (bottom).

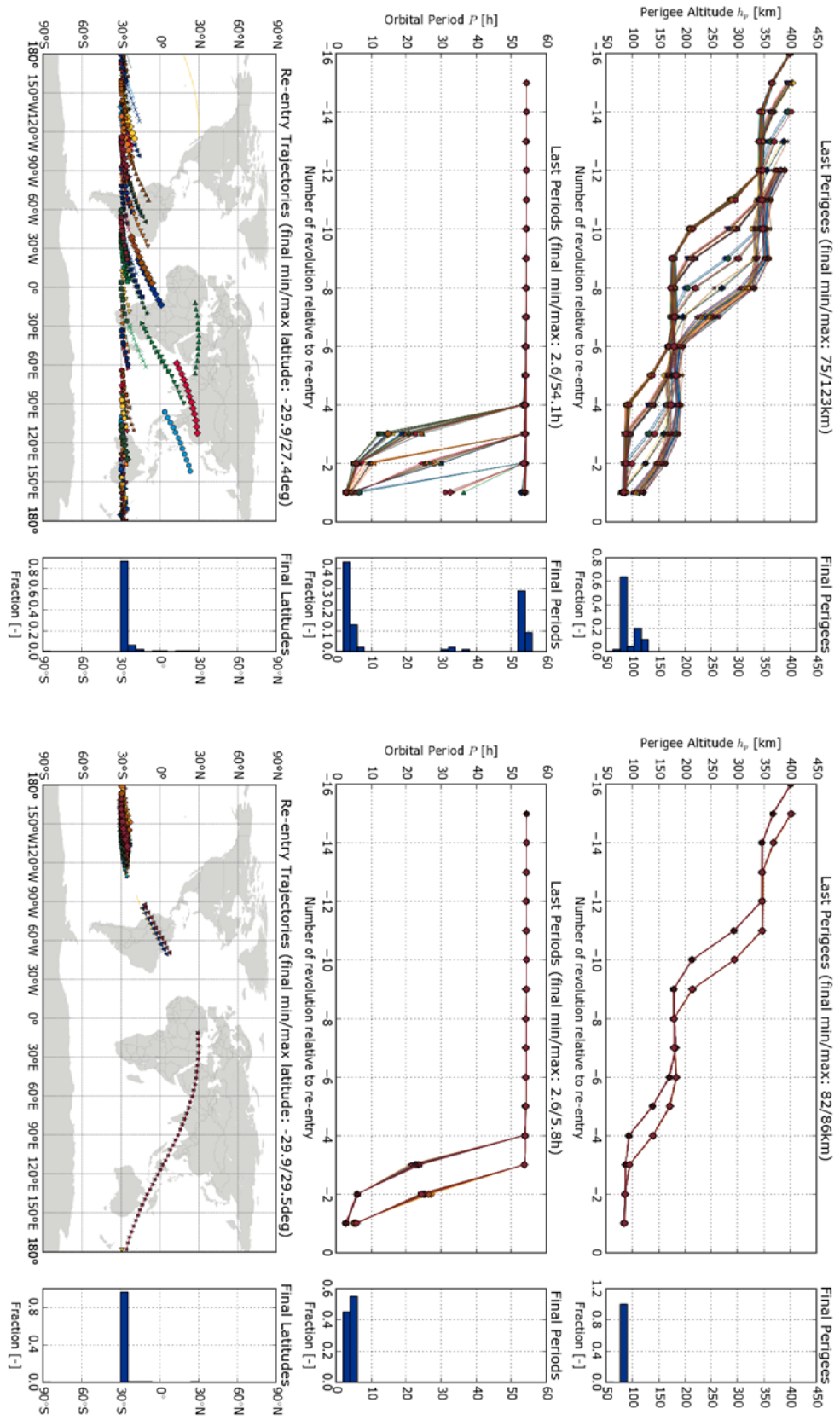

Figure 12: Re-entry longitude analysis for Cluster-2, starting from January 2017 (top) and July 2024 (bottom).

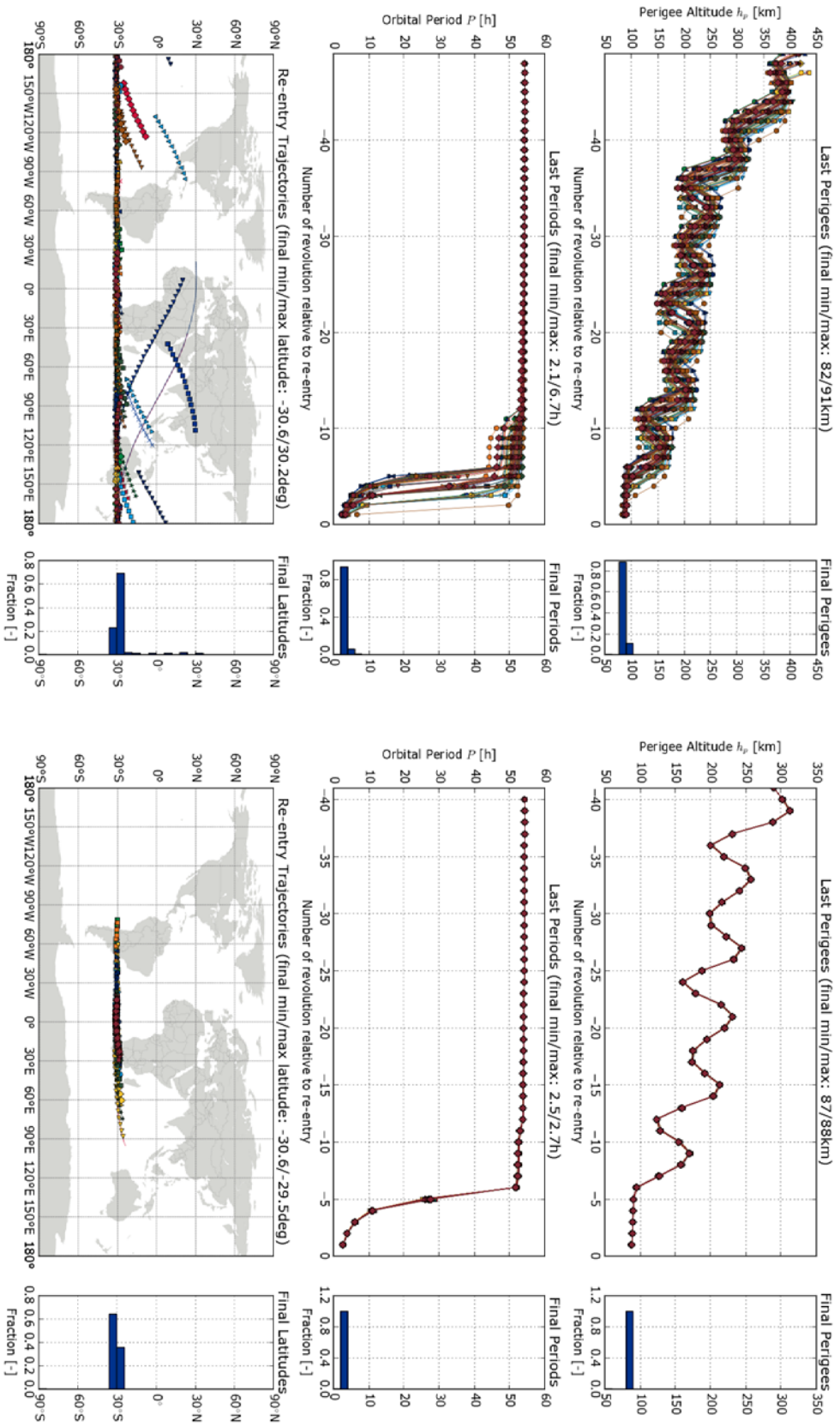

Figure 13: Re-entry longitude analysis for Cluster-3, starting from January 2017 (top) and June 2026 (bottom).

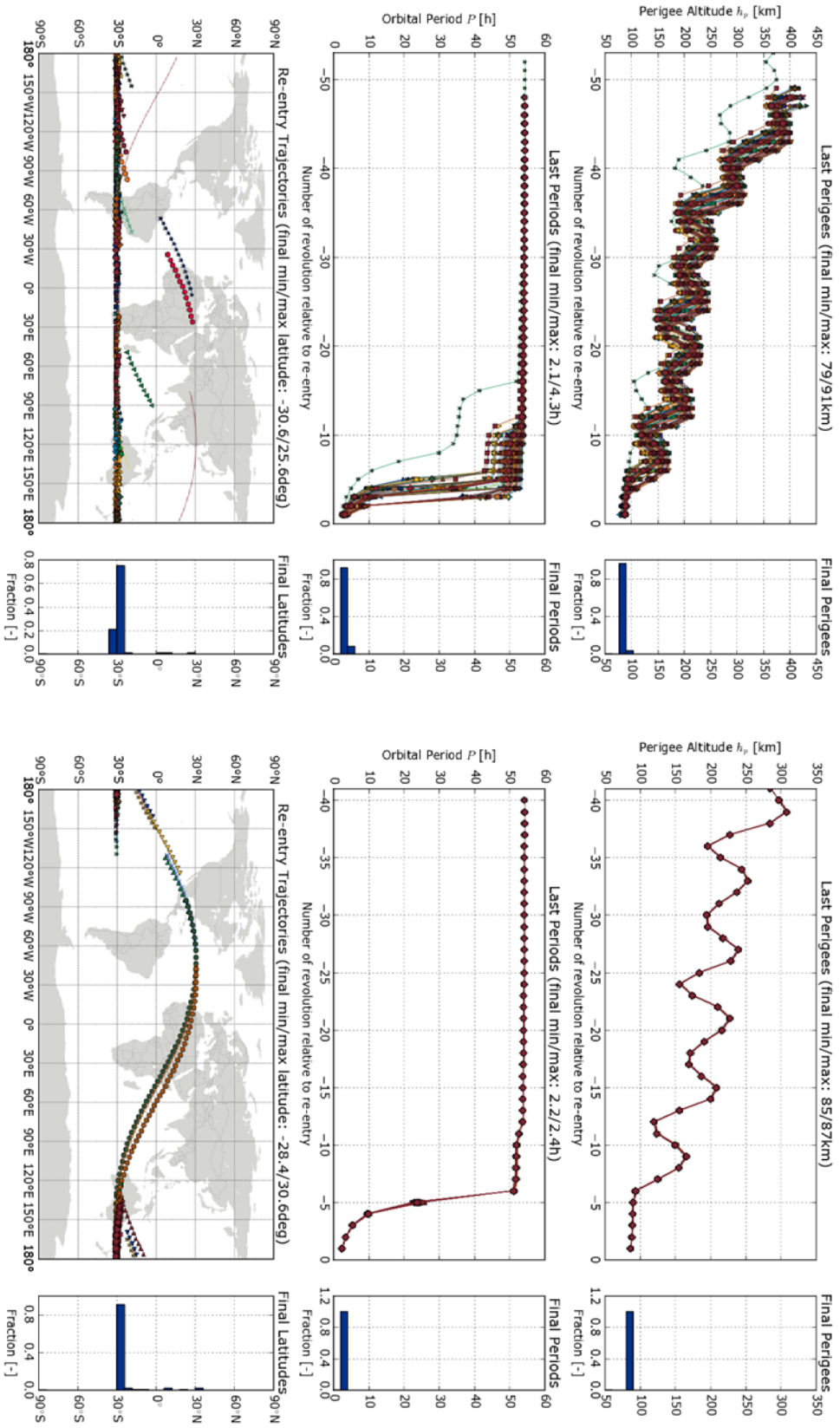

Figure 14: Re-entry longitude analysis for Cluster-4, starting from January 2017 (top) and June 2026 (bottom)